doi:10.3772/j.issn.1006-6748.2023.02.008

Paired regions for shadow removal approach based on multi-features①

ZHANG Zhizheng(张之政)[*,**,***], GUO Mingqiang②[*,**,***], WU Liang[**,***], HUANG Ying[****], CHEN Xueye[*]

([*] Key Laboratory of Urban Land Resources Monitoring and Simulation, Ministry of Natural Resources, Shenzhen 518034, P. R. China)

([**] National Engineering Research Center of Geographic Information System, China University of Geosciences, Wuhan 430074, P. R. China)

([***] School of Computer Science, China University of Geosciences, Wuhan 430074, P. R. China)

([****] Wuhan Zondy Cyber Technology Co., Ltd., Wuhan 430074, P. R. China)

Abstract

The existence of shadow leads to the degradation of the image qualities and the defect of ground object information. Shadow removal is therefore an essential research topic in image processing filed. The biggest challenge of shadow removal is how to restore the content of shadow areas correctly while removing the shadow in the image. Paired regions for shadow removal approach based on multi-features is proposed, in which shadow removal is only performed on related sunlit areas. Feature distance between regions is calculated to find the optimal paired regions with considering of multi-features (texture, gradient feature, etc.) comprehensively. Images in different scenes with peak signal-to-noise ratio (PSNR) and structural similarity (SSIM) evaluation indexes are chosen for experiments. The results are shown with six existing comparison methods by visual and quantitative assessments, which verified that the proposed method shows excellent shadow removal effect, the brightness, color of the removed shadow area, and the surrounding non-shadow area can be naturally fused.

Keywords: paired region, feature distance, texture, peak signal-to-noise ratio (PSNR), structural similarity (SSIM)

0 Introduction

Shadow removal is an important prerequisite for visual processing of images, such as object recognition and moving object tracking. The existence of shadow in the image leads to the defect of ground object information, which reduces the accuracy of image interpretation and seriously affects various quantitative analysis and application. Therefore, the extraction of the shadow area in the image is an essential step for the subsequent image processing. At the same time, the biggest challenge of shadow removal is how to restore the texture details of shadow areas while removing the shadow, so that the brightness and color of the restored shadow area and the surrounding non-shadow area can be naturally fused.

Existing shadow removal technologies can be roughly divided into three aspects: gamma correction method[1-3], illumination transfer technology[4-8], and deep learning model[9-12].

The gamma correction method mainly uses the color features or statistical characteristics of the illumination area to construct the illumination recovery factor, so as to correct the shaded area. Ref. [1] divided the shadow into umbra and penumbra, and proposed a shadow removal method based on multi-channel gamma correction and shadow depth map. Ref. [2] used the color sampling line of the illumination area to offset and correct shadow areas. Ref. [3] used Shearlet approximation coefficients to correct shaded pixels and eventually generated shade-free pixels.

Secondly, the illumination transfer method is also one of the research hotspots. Ref. [4] calculated the illumination compensation coefficient by using the illumination area adjacent to the shadow boundary, and finally compensated shadow areas. Ref. [5] proposed a shadow removal method based on light component correction. Ref. [6] calculated the average intensity ratio between sunlit area and the shadow area in R(red), G(green) and B(blue) channels respectively, and compensates the shadow pixel by pixel. Based on the sim-

① Supported by the National Natural Science Foundation of China (No. 41971356, 41701446) and the Open Fund of Key Laboratory of Urban Land Resources Monitoring and Simulation, Ministry of Natural Resources (No. KF-2022-07-001).

② To whom correspondence should be addressed. E-mail: gmqandjxs@163.com.

Received on July 25, 2022

plified physical illumination model and image decomposition formula, Ref. [7] constructed linear transformation functions in each channel of RGB of the original image by using shadow areas and sunlit regions. The shadow removal is realized by estimating the parameter value of the function. Ref. [8] added a constant offset according to the chrome difference and surface characteristics of the shadow in the lab color space on the basis of the super-pixel segmentation, and finally realized the illumination compensation of the shadow.

With the rapid development of deep learning technology in recent years, many scholars use classical models of deep learning to shadow removal and achieve very good results. According to the physical characteristics of shadows and the imaging principle of cameras, Ref. [9] comprehensively considered the relationship between color channels and proposed a generative adversarial network based on multi-channel attention mechanism to achieve shadow removal based on deep learning methods. Ref. [10] constructed a convolutional neural network based on knowledge transfer. Under the guidance of shadow-free images, the shadow removal process can be realized without shadow detection. Ref. [11] proposed a multi-task generative adversarial network, which utilizes the crossover trajectory module to learn the fusion and constraint characteristics between multiple tasks, and can simultaneously detect and eliminate shadows. In view of the problem that deep neural network lost a large amount of feature information in the process of image normalization, Ref. [12] proposed a spatial adaptive de-normalization method to prevent the loss of spatial features of input image data, so as to accurately remove shadow areas. However, deep learning-based methods often need to artificially construct a group of shadow images and shadow-free images correspondingly, which requires a large amount of time. In addition, due to the changes in camera exposure, posture and ambient illumination, the color, illumination or spatial location of images may change when constructing paired sample sets, which may lead to the errors in learning the nonlinear relationship between shadows and non-shadows.

It has been long-term research for shadow removal by restoring the image information in the shadow area. Through the above analysis, the problem encountered is as follows. How to restore the texture details of shadow area while eliminating the shadow, so as to make the brightness and color of the restored shadow areas naturally merge with the surrounding sunlit areas. Therefore, paired regions for shadow removal approach based on multi-features is proposed.

The rest of this article is organized as follows. Section 1 describes the correlation method of shadow removal based on block matching. In Section 2, a series of experiments are given to prove the effectiveness and performance of the proposed method. Section 3 gives conclusions and future work.

1 Methods

The framework of the proposed method is shown in Fig. 1.

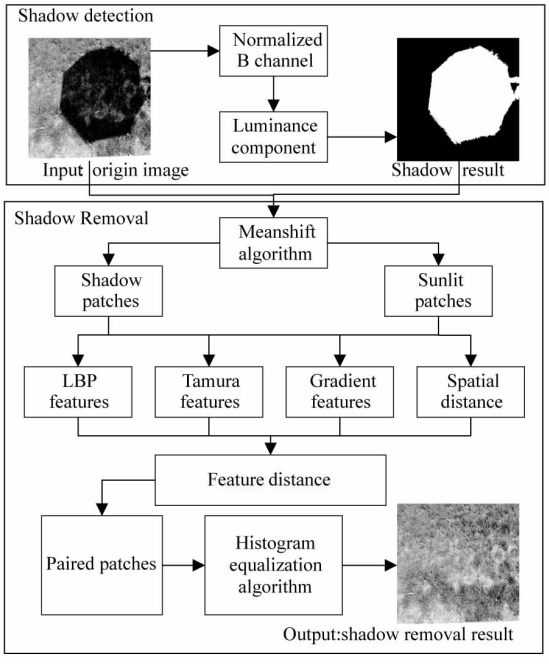

Fig. 1 The framework of the proposed method

1.1 Shadow detection

The extraction of shadow area in image is an essential step for shadow removal. The brightness of the shadow areas is low because the light is blocked. Through the analysis of Phong lighting model[13], it was found that B channel in shadow areas dropped least among the three RGB channels. Therefore, in the normalized B component, the shadow occupies the high pixel value end, so a threshold can be set to obtain a rough shadow area. To sum up, only regions above a certain threshold in the normalized B component and below a certain threshold in the luminance component are detected as shadow.

In terms of shadow detection, the inter-class variance formula is used to calculate the segmentation threshold in this paper. Shadow detection itself is a pixel-level image binary classification task, and the inter-class variance formula is a method to divide the image into foreground and background according to the gray

characteristics of the image. The maximum inter-class variance means the minimum misclassification probability. The inter-class variance formula is as follows.

$$g = w_0 \times (\mu_0 - \mu)^2 + w_1 \times (\mu_1 - \mu)^2 \quad (1)$$

where g represents the inter-class variance, w_0 represents the proportion of shadow pixels in the overall image, w_1 represents the proportion of non-shadow pixels in the overall image, μ_0 represents the average gray value in the shadow image, μ_1 represents the average gray value in the non-shadow image, μ represents the average gray value of the whole image, which can be expressed as $\mu = w_0\mu_0 + w_1\mu_1$.

1.2 Image segmentation

Before the shadow removal operation, the plots in the shadow area and sunlit area need to be carefully segmented so that each region after segmentation contains only one kind of object. In practical, it is necessary to segment shadow areas and sunlit area respectively, so as to extract the regions in an image in a more detailed way. The advantage of mean-shift algorithm is that the number of clustering does not need to be set in advance. The application of mean-shift algorithm in images can also be regarded as the task of image clustering. First, an image needs to be converted from RGB color space to LUV color space. Secondly, according to initial clustering center $y_{i,j}$ of the image, the spatial position and LUV space are combined to form a 5-dimensional vector $\boldsymbol{y}_{i,j} = (i, j, L_{i,j}, u_{i,j}, v_{i,j})$. Finally, the kernel function $g(\ )$ is used to calculate new clustering center $\boldsymbol{y}_{i,j}' = (\bar{i}, \bar{j}, \overline{L_{i,j}}, \overline{u_{i,j}}, \overline{v_{i,j}})$. The calculation formulas of new spatial coordinates $(\bar{i}, \bar{j})$ and color components $(\overline{L_{i,j}}, \overline{u_{i,j}}, \overline{v_{i,j}})$ of the cluster center $\boldsymbol{y}_{i,j}'$ are as follows.

$$\bar{i} = \frac{\sum_{k=1}^{N} i \times g\left(\left(\frac{i_k - i}{h_s}\right)^2\right)}{\sum_{k=1}^{N} g\left(\left(\frac{i_k - i}{h_s}\right)^2\right)} \quad (2)$$

$$\bar{j} = \frac{\sum_{k=1}^{N} j \times g\left(\left(\frac{j_k - j}{h_s}\right)^2\right)}{\sum_{k=1}^{N} g\left(\left(\frac{j_k - j}{h_s}\right)^2\right)} \quad (3)$$

$$\overline{L_{i,j}} = \frac{\sum_{k=1}^{N} L_{i,j} \times g\left(\left(\frac{L_k - L_{i,j}}{h_r}\right)^2\right)}{\sum_{k=1}^{N} g\left(\left(\frac{L_k - L_{i,j}}{h_r}\right)^2\right)} \quad (4)$$

$$\overline{u_{i,j}} = \frac{\sum_{k=1}^{N} u_{i,j} \times g\left(\left(\frac{u_k - u_{i,j}}{h_r}\right)^2\right)}{\sum_{k=1}^{N} g\left(\left(\frac{u_k - u_{i,j}}{h_r}\right)^2\right)} \quad (5)$$

$$\overline{v_{i,j}} = \frac{\sum_{k=1}^{N} v_{i,j} \times g\left(\left(\frac{v_k - v_{i,j}}{h_r}\right)^2\right)}{\sum_{k=1}^{N} g\left(\left(\frac{v_k - v_{i,j}}{h_r}\right)^2\right)} \quad (6)$$

where, h_s is the space threshold; h_r is the color threshold; i_k, j_k, L_k, u_k and $v_k (k = 1, 2, \cdots, N)$ are the spatial coordinate and color value of the k – th pixel in the defined region Ω according to h_s and h_r; N is the total number of numbers in region Ω; and $g(\ )$ is the kernel function.

When the new clustering center $\boldsymbol{y}_{i,j}'$ is obtained, the mean shift vector can be obtained, and the formula is as follows.

$$ms_{\text{shift}} = \boldsymbol{y}_{i,j}' - \boldsymbol{y}_{i,j} \quad (7)$$

Until the convergence condition $\|ms_{\text{shift}}\| < \varepsilon$ is satisfied, the clustering process does not end up. As the same object in the image has similar material and color, the whole image is finally divided into irregular blocks according to spatial distance and color distance through clustering, and each block contains only one kind of ground objects.

1.3 Establishment of region matching rules

When the image is segmented, for each shadow block in shadow, it is necessary to find the most similar block in sunlit area. First, according to the first law of geography, the correlation between objects is related to distance. In general, the closer the distance, the greater the correlation between features. Considering the spatial correlation between ground objects, it is necessary to select the sunlit block close to the shadow block according to the spatial distance.

A ground object in shadow and sunlit conditions will take on different colors due to the influence oflight. So, the criteria which is built for block matching should be light independent. About the matching of shadow block and illumination block, this paper considers from two aspects comprehensively: texture feature and gradient feature.

Local binary pattern (LBP) is a simple and effective method to describe non-parametric local texture features. It can be used to extract the details of images and represent the surface structure characteristics of

objects. At the same time, it can effectively resist the interference of light. In order to cope with the problem of different image sizes and meet the requirements of gray scale and rotation invariance at the same time, Ojala et al. [14] improved the original LBP operator by changing the original 3×3 rectangle operator into a circular LBP operator taking sampling radius R and sampling point P as parameters of Ref. [14].

A center point is denoted as (x_c, y_c), and its surrounding pixels are denoted as (x_p, y_p), $p \in P$. The calculation formula of sampling point is

$$\begin{cases} x_p = x_c + R\cos\left(\dfrac{2\pi p}{P}\right) \\ y_p = y_c - R\sin\left(\dfrac{2\pi p}{P}\right) \end{cases} \tag{8}$$

where, R is the radius of LBP operator, p is the p-th sampling point, and P is the total number of sampling points. In order to extract texture features, the modified LBP operator is used to describe local texture features of images. Considering rotation invariance, the image is divided into eight directions according to 45°, the local binary mode of each direction is taken, and the minimum value is taken as the LBP value of the center.

This paper also considers roughness and contrast in Tamura texture features to characterize texture properties. Image roughness is the most important feature of texture features, which can best represent the content of texture features and reflect the change speed of image gray value. It is necessary for each pixel (x, y) to calculate the average intensity value in the $2^k \times 2^k$ window with this pixel as the center.

$$I_k(x, y) = \frac{1}{2^{2k}} \sum_{i=x-2^{k-1}}^{x+2^{k-1}} \sum_{j=y-2^{k-1}}^{y+2^{k-1}} f(i, j) \tag{9}$$

In Eq. (9), $f(i, j)$ represents the gray value located there. Then calculate the average intensity difference for each pixel in the vertical and horizontal directions, and the calculation formula is as follows.

$$\begin{cases} E_{k,h} = |I_k(x + 2^{k-1}, y) - I_k(x - 2^{k-1}, y)| \\ E_{k,v} = |I_k(x, y + 2^{k-1}) - I_k(x, y - 2^{k-1})| \end{cases} \tag{10}$$

$$E_{\text{best}}(x, y) = \max(E_{k,h}, E_{k,v}) \tag{11}$$

In Eqs(10) and (11), $E_{k,h}$ represents the average intensity difference of each pixel in the horizontal direction, and $E_{k,v}$ represents the pixel difference of each pixel in the vertical direction. In addition, the optimal size of pixel point (x,y) should be set to E_{best}. Thus, centering on pixel point(x,y), the average value of $\bar{E}_{\text{best}}$ is calculated as a quantitative index of texture roughness. The specific calculation formula is

$$F_{\text{coarseness}}(i, j) = \frac{1}{m \times n} \sum_{i=1}^{m} \sum_{j=1}^{n} |E_{\text{best}}(i, j) - \overline{E_{\text{best}}}(i, j)| \tag{12}$$

Contrast, on the other hand, describes the brightness of the image, which can reflect the sharpness and depth ofthe texture of the image. The specific expression formula is

$$\alpha_4 = \frac{\mu_4}{\sigma^4} \tag{13}$$

$$F_{\text{contrast}} = \frac{\sigma}{\alpha_4^{1/4}} \tag{14}$$

where, μ_4 represents the fourth-order moment of image gray scale, σ is the standard deviation of image gray scale, and α_4 represents the fourth-order standard moment of image.

Image gradient refers to the changes in the direction of image intensity and color. The calculation formula of image function gradient is shown as follows.

$$\nabla f(x, y) = [G_x, G_y]^{\mathrm{T}} = \left[\frac{\partial f}{\partial x}, \frac{\partial f}{\partial y}\right]^{\mathrm{T}} \tag{7}$$

$$mag(\nabla f) = g(x, y) = \sqrt{\frac{\partial^2 f}{\partial x^2} + \frac{\partial^2 f}{\partial y^2}} \tag{8}$$

In Eqs(15) and (16), G_x represents the gradient value of the image in the horizontal direction, G_y represents the gradient value of the image in the vertical direction, and $g(x, y)$ represents the gradient of the image at the point (x, y).

Calculation of feature distance between regions. If shadow patch A and sunlit patch B are the same ground object, they have spatial correlation and similarity in texture features and gradient features. Combined with the above analysis, this paper constructs the feature distance between shadow patches and sunlit patches. Formulas are listed as follows.

$$Total_{\text{dis}} = Texture_{\text{dis}} + Gradient_{\text{dis}} + Spatial_{\text{dis}} \tag{9}$$

$$Texture_{\text{dis}} = \| LBP_A - LBP_B \|_2 + \| F_{\text{coarseness}_A} - F_{\text{coarseness}_B} \|_2 + \| F_{\text{contrast}_A} - F_{\text{contrast}_B} \|_2 \tag{10}$$

$$Gradient_{\text{dis}} = \| g_A - g_B \|_2 \tag{11}$$

$$Spatial_{\text{dis}} = \sqrt{(x_A - x_B)^2 + (y_A - y_B)^2} \tag{12}$$

When feature distance $Total_{\text{dis}}$ is small, it means that shadow patch A and sunlit patch B are similar and can be regarded as the same ground object.

1.4 Shadow removal

When shadows in the image find matching sunlit regions, it needs to use the relevant sunlit regions to remove shadow. The specific method is to use the histogram equalization method. Histogram equalization algorithm achieves the purpose of image enhancement by counting the gray value of pixels and stretching the histogram. The process of performing histogram equalization on a color image is to first decompose the color image into several channels. The probability of the $k-$th gray level can be expressed as

$$P_r(r_k)=\frac{n_k}{n},\ k=0,1,2,\cdots,L-1 \tag{13}$$

where, n is the total number of pixels and L is the total number of gray levels.

After histogram equalization of the image f, the pixel whose gray level is r_k can be modified to S_k by transformation function γ.

$$S_k=\gamma(r_k)=\sum_{i=1}^{k}P_r(r_i)=\sum_{i=1}^{k}\frac{n_i}{n} \tag{14}$$

Secondly, the number of pixels n'_k of the new gray level S_k after mapping is counted

$$n'_k=255\times S_k \tag{15}$$

The equalization operation is performed on these channels respectively, and finally all channels are merged to generate a new image. Therefore, the histogram equalization method is used to restore the illumination and texture details of shadow areas.

2 Experiments

2.1 Experimental environment and dataset description

In this part, the qualitative and quantitative assessments of the proposed approach are evaluated on public datasets. The Image Shadow Triplets Dataset (ISTD) is used as the benchmark to compare the performances of different shadow-detection methods. ISTD is a dataset for shadow understanding that contains 1870 image triplets of shadow image, shadow mask, and shadow-free image. ISTD datasets can be obtained from https://paperswithcode.com/dataset/istd.

For the shadow removal methods, the proposed approach is compared with popular classic methods. Classical methods include illumination ratio (IR)[15], linear correction (LC)[16], Poisson equation (Poisson)[17], low illumination map estimation (LIME)[18], adjacent objects compensation (Zhou's)[4], region matching and mapping function optimization (RMMFO)[19].

Peak signal-to-noise ratio (PSNR) is the most common and widely used index to measure image quality. Structural similarity (SSIM) refers to structural similarity index, which is to measure the similarity of two images. The indices of the PSNR and SSIM are introduced to make the comparison reliable and to evaluate these methods quantitatively.

2.2 Experiments and performance assessments

In order to verify the shadow removal effect of the proposed method in different scenes, several groups of images are selected for experiments. It can be seen from Fig. 2 that after shadow removal, the grass, stone piles, tree trunks and bare ground that were originally blocked by shadow retain their original color and material information. The method in this paper has achieved excellent shadow removal effect in different scenes, and the restored image and the illumination area have achieved natural fusion.

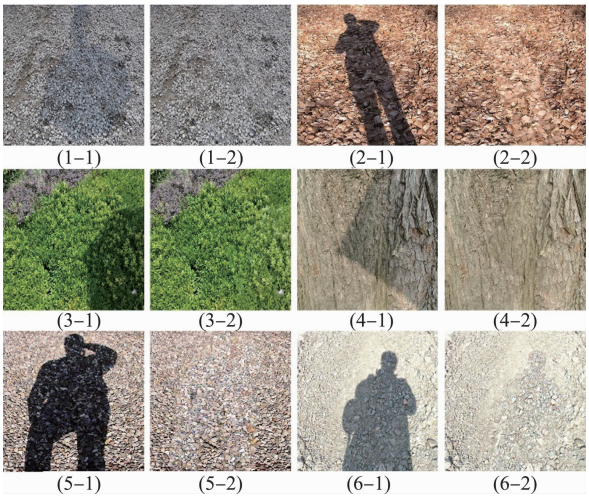

Fig. 2 Shadow removal results of the proposed method in different scenes

Furthermore, images in road and vegetation scenarios are chosen to evaluate the outstanding shadow removal performance of the proposed method with comparison methods.

Fig. 3 shows shadow removal results of these methods in road scene. For Poisson method, LIME method and LC method, the shaded areas show color differences in Fig. 3 (b), (c) and (d). It can be seen from Table 1 that the PNSR values of the two methods are very low, which means that the image reconstruction

effect is poor. The SSIM values of the two methods are below 0.83, which means that images after shadow removal have little similarity with original shadow-free images. There is no distortion in IR method, Zhou's method and RFFMO method, but the brightness after shadow removal is not consistent with the surrounding illumination area, as shown in Fig. 3 (e), (f) and (g). However, the brightness and color of restored shadow area and the surrounding non-shaded area are naturally fused with the proposed method. It can also be seen from Table 1 that PNSR and SSIM of the proposed method in this paper are the highest, reaching 24.30 and 0.8664 respectively. The method in this paper has the best reconstruction effect in shadow area, and the image after shadow removal is the most similar to the original shadow free image, as shown in Fig. 3(h).

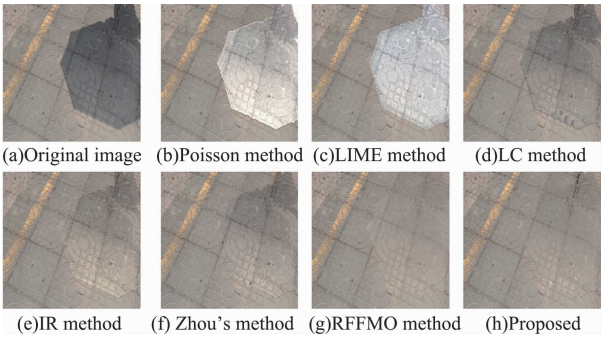

Fig. 3 Shadow removal results of these methods in road scene

Fig. 4 shows shadow removal results of these methods in vegetation scenario. For LC and Zhou's method in Fig. 4(d) and (f), the brightness of shadow edge is low and distortion occurs inside the shadow. However, as for Poisson method and LIME method, the color of grass in the shadow area is inconsistent with the sunlit area, as shown in Fig. 4(b) and (c). PSNR is small in Table 2, resulting in poor removal effect. In addition, there is a significant color difference at the boundary after shadow removal for the IR method in Fig. 4. The orange patches appear distorted after shadow removal with RMMFO method as shown in Fig. 4 (g). As for the proposed method, the grass inside shadow has the same color as the grass in sunlit area in Fig. 4(h). The shadow and sunlit area naturally merge at the boundary. It can be seen from Table 2 that SSIM value reaches 0.82 and the PSNR value is the highest, which means that the proposed method shows excellent shadow removal effect in the vegetation scene, and the result after removal is similar to the original shadow-free image.

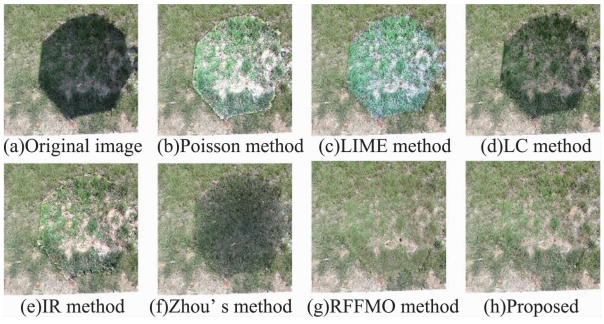

Fig. 4 Shadow removal results of these methods in vegetation scene

Table 1 PSNR and SSIM evaluation index in Fig. 3

	Poisson	LIME	LC	IR	Zhou	RFFMO	Proposed
PSNR	16.18	15.88	22.68	23.04	23.33	23.95	24.32
SSIM	0.7987	0.6946	0.8228	0.8488	0.8525	0.8604	0.8664

Table 2 PSNR and SSIM evaluation index in Fig. 4

	Poisson	LIME	LC	IR	Zhou	RFFMO	Proposed
PSNR	13.99	14.66	15.32	16.32	15.47	16.80	21.67
SSIM	0.7634	0.7450	0.7901	0.8094	0.7581	0.8039	0.8191

3 Conclusion

In this study, paired regions for shadow-removal approach based on multi-features is developed. Block matching rules for shadow removal is established in accordance with multi-features (texture, gradient feature, etc.) comprehensively. The designed combination of feature distance between blocks can eliminate the shadows in images effectively. Compared with other shadow removal methods from the qualitative and quantitative analyses, the superiority of the proposed method in shadow removal are verified with the highest PSNR and SSIM values. The proposed method shows excellent shadow removal effect in different scenes, and the result after removal is similar to the original shadow-free image.

The proposed method can effectively remove the shadow area in the image only by inputting a single image. However, the shadow removal method proposed in this study fails to further consider the processing of the penumbra region at the shadow boundary. In future work, the addition of other spectral band and complex scenes

can be considered. Furthermore, future work will focus on the process of penumbra region. Shadow removal and image interpretation by incorporating the spectral and spatial information will be the focus of future research.

References

[1] PARK K H, LEE Y S. Simple shadow removal using shadow depth map and illumination-invariant feature[J]. Journal of Supercomputing, 2022, 78(3):4487-4502.

[2] ZHU T J, ZOU Z W, WU T L, et al. Shadow removal method for single image based on instant learning[J]. Sensors and Materials, 2021, 33(8):2693-2708.

[3] MURALI S, GOVINDAN V K, KALADY S. Shadow removal from uniform-textured images using iterative thresholding of shearlet coefficients [J]. Multimedia Tools and Applications, 2019, 78(15):21167-21186.

[4] ZHOU T T, FU H Y, SUN, C L, et al. Shadow detection and compensation from remote sensing images under complex urban conditions[J]. Remote Sensing, 2021, 13(4):699.

[5] LUO S, SHEN H F, LI H F, et al., Shadow removal based on separated illumination correction for urban aerial remote sensing images[J]. Signal Processing, 2019, 165:197-208.

[6] Amin B, Riaz M M, Ghafoor A. Automatic shadow detection and removal using image matting[J]. Signal Processing, 2020, 170(2):107415.

[7] LE H, SAMARAS D. Shadow removal via shadow image decomposition[C]//2019 IEEE/CVF International Conference on Computer Vision (ICCV). Seoul:IEEE, 2019:8577-8586.

[8] XU W Y, CHEN H, SU Q, et al. Shadow detection and removal in apple image segmentation under natural light conditions using an ultrametric contour map[J]. Biosystems Engineering, 2019, 184:142-154.

[9] ABIKO R, IKEHARA M, Channel attention GAN trained with enhanced dataset for single-image shadow removal[J]. IEEE Access, 2022, 10:12322-12333.

[10] SANG Y, ZHANG S H, HE H, et al., Brightness-gradient difference feature guided shadow removal method[J]. Knowledge-based Systems, 2022, 239:107986.

[11] JIANG X Y, HU Z Y, NI Y, et al. Shadow detection and removal based on multi-task generative adversarial networks [C]// The 11th International Conference on Image and Graphics (ICIG 2021). Haikou: Springer, 2021:366-376.

[12] RYU H, KIM T, CHOE Y. Single image shadow removal via detection-free spatially adaptive denormalization[C]//2021 International Workshop on Advanced Imaging Technology (IWAIT). Virtual:SPIE, 2021.

[13] Novotny P M, Ferrier N J. Using infrared sensors and the Phong illumination model to measure distances[C]//IEEE International Conference on Robotics and Automation. Detroi: IEEE, 1999:1644-1649.

[14] OJALA T, PIETIK-INEN M, HARWOOD D. A comparative study of texture measures with classification based on featured distributions[J]. Pattern Recognition, 1996, 29(1): 51-59.

[15] SILVAG F, CARNEIRO G B, DOTH R, et al. Near real-time shadow detection and removal in aerial motion imagery application[J]. ISPRS Journal of Photogrammetry and Remote Sensing, 2018, 140:104-121.

[16] SUNY A, MITHILA N M, A shadow detection and removal from a single image using LAB color space[C]//International Journal of Computer Science Issues (IJCSI), Russia, 2013, 10:95-103.

[17] FINLAYSON G D, DREW M S,LU C. Entropy minimization for shadow removal[J]. International Journal of Computer Vision, 2009, 85(1):35-57.

[18] GUO X. LIME:a method for low-light image enhancement[C]//Proceedings of the 24th ACM International Conference on Multimedia. New York:Association for Computing Machinery, 2016:87-91.

[19] HSIEH S W, YANG C H, LU Y C. Shadow removal through learning-based region matching and mapping function optimization [C]//2022 IEEE International Conference on Multimedia and Expo (ICME). Taibei:IEEE, 2022:1-6.

ZHANG Zhizheng, born in 1997. He received his B. S. degree in China University of Petroleum (Beijing) in 2019. He also received his M. S. degree in National Engineering Research Center of Geographic Information System from China University of Geosciences (Wuhan) in 2023. His research interests include image processing and computer vision.